Int J Adv Manuf Technol
DOI 10.1007/s00170-016-9674-1

ORIGINAL ARTICLE

Process control model for growth rate of molecular beam epitaxy of MgO (111) nanoscale thin films on 6H-SiC (0001) substrates

Ghulam Moeen Uddin[1] · **Katherine S. Ziemer**[2] · **Abe Zeid**[1] · **Yung-Tsun Tina Lee**[3] · **Sagar Kamarthi**[1]

Received: 1 July 2016 / Accepted: 28 October 2016

Abstract Magnesium oxide (MgO) is a good candidate for an interface layer in multifunctional metal-oxide nanoscale thin-film heterostructures due to its high breakdown field and compatibility with complex oxides through O bonding. In this research, molecular beam epitaxy (MBE) is used to deposit 10 nm to 15 nm MgO single-crystal films on silicon carbide with hexagonal polytype 6H (6H-SiC) to serve as an interface layer for effective integration of functional oxides. In this work, the effect of MBE process control variables on the growth rate of the MgO film measured in nanometers per minute is investigated. Experiments are conducted at various process conditions and the resulting MgO film growth rate at each combination of process conditions is measured. The process control variables studied are the substrate temperature (100 °C – 300 °C), magnesium source temperature (328 °C – 350 °C), plasma intensity (0 mV – 550 mV), and percentage oxygen on the starting surface of 6H-SiC substrate (9 % – 13 %) after the substrate is prepared by high-temperature hydrogen etching. The film thickness is computed using the effective attenuation length (EAL) of silicon photoelectron peak intensity as measured by x-ray photoelectron spectroscopy (XPS). The film thickness is converted to growth rate by dividing it with the duration of film growth. Using the experimental data, a neural network model is developed to estimate growth rate for any given process variable combination. From this neural network model, multiple replications of data were generated to conduct a 3-level full factorial design of experiments and response surface-based analysis. The study reveals that the plasma intensity has the most significant influence on growth rate. The results indicate that growth rate is relatively low on high-quality substrates with $\sqrt{3} \times \sqrt{3}$ R30° reconstructed 6H-SiC (0001) surface with optimum oxygen content (approximately 10 %); in contrast, the growth rate is relatively high on substrates with high surface roughness and excessive oxygen on the starting substrate surface.

Keywords Nanoscale manufacturing · Manufacturing process modeling · Molecular beam epitaxy · Magnesium oxide nanoscale thin films · Functional oxide heterostructures · Neural networks · Interface engineering · Data analytic · Smart manufacturing

1 Introduction

Much research in the field of next-generation nanoscale devices is based on vertically stacked multifunctional metal-oxide nanoscale thin-film heterostructures, such as the integration of perovskite ferroelectrics like barium titanate (BTO) and hexagonal ferrites like barium hexaferrite (BaM) on semiconductor substrates [1, 2]. The control over the processing parameters of the molecular beam epitaxy (MBE) process is critical to the quality and growth rate of the MgO thin films. Many research groups have investigated the relation between the quality of MgO thin films and processing parameters, but the relation of processing parameters and the growth rate of MgO thin films has not been investigated yet. Craft et al. [3] studied the impact of the critical parameters such as substrate temperature, magnesium effusion cell temperature, and oxygen pressure in the MBE chamber on the crystal structure

✉ Sagar Kamarthi
Sagar@coe.neu.edu

[1] Department of Mechanical and Industrial Engineering, Northeastern University, Boston, MA 02115, USA

[2] Chemical Engineering Department, Northeastern University, Boston, MA 02115, USA

[3] National Institute of Standards and Technology, 100 Bureau Dr, Gaithersburg, MD 20899, USA

Published online: 30 November 2016

quality of MgO thin films grown on GaN substrates. Chen et al. [4] demonstrated the growth of high-quality single-crystal MgO (111) thin films on SiC substrates by controlling substrate temperature, oxygen pressure in the MBE chamber, and temperature of magnesium effusion cells. MgO (111) (the magnesium oxide 111 surface) thin film template-assisted growth of these functional oxide nanoscale thin films—with excellent chemical and crystalline uniformity—on wide band gap silicon carbide with hexagonal polytype 6H (6H-SiC) (0001) have been demonstrated by various researchers [5–8]. Again, the quality of the MgO thin films was reported to be dependent upon tight control on the parameters, such as substrate temperature, temperature of the magnesium effusion cells, oxygen plasma pressure in the chamber, and plasma intensity.

The MgO (111) template interface helps reduce the structural mismatch between 6H-SiC (0001) substrates and the more complex metal-oxide functional films due to the pseudo hexagonal structure of the 111 face and the oxygen–oxygen atom spacing in the MgO. The integrity of the crystalline structure of the MgO (111) film is very closely related to its atomic composition, and both are very sensitive to the (a) process control variables of the MBE system and (b) thickness of the film. In particular, the structural strain mismatch i.e., tensile strain in the <110> direction and compressive strain in the <112> direction causes an inherent twist in the growth of MgO (111) films. This structural strain mismatch is a key concern to the single-crystal character of the films as they grow thicker [9].

When subject to high temperature hydrogen cleaning process, the 6H-SiC (0001) substrate surface is terminated by a ($\sqrt{3} \times \sqrt{3}$) R30° reconstruction, which contains a silicate adlayer [9–13]. The pseudo hexagonal atomic arrangement in the silicate adlayer on the 6H-SiC (0001) and MgO (111) plane are shown in Fig. 1. The oxygen atoms of the MgO (111) film monolayer overlay the 6H-SiC (0001) surface with a 3.3 % tensile mismatch [2]. The response of the structural strain in the <110> and <112> directions is tensile and compressive, respectively [9].

The 3.3 % lattice mismatch between MgO and SiC is complicated by any additional strain introduced by the MgO film deposition process in response to the process control variables, such as substrate temperature, magnesium source temperature, plasma intensity, and percentage starting oxygen content. Previous research by the authors' research group has shown that under optimal processing conditions, two-dimensional-growth can be maintained for up to 15 nm to 20 nm. Once the film is 30 nm thick or more, the film shows three-dimensional quality as indicated by reflection high-energy electron diffraction (RHEED), surface roughness from atomic force microscopy, and cross-sectional imaging by tunneling electron microscopy [3]. Thus, the thickness of the film is a critical dimension for ensuring that the MgO (111) film is an effective template layer to integrate a functional oxide on 6H-SiC substrates. This is the primary reason why the relationship between the process control variables and the growth rate of the MgO (111) films is studied in this work.

In this work, a neural network-assisted response surface-based analysis was conducted to understand the dynamics and interplay between the growth rate and quality of an MgO film grown on 6H-SiC substrate in response to the changes in MBE process control variables. In this study, film quality is characterized by crystallinity of the film (single-crystal 111 orientation) through RHEED and atomic concentration and Mg–O bonding states as determined by X-ray photoelectron spectroscopy (XPS).

2 Experimental procedure

Film deposition experiments were conducted using the ultra-high vacuum (UHV) chamber shown in Fig. 2. There is a connected UHV analysis chamber containing the XPS, to which the sample can be transferred without exposure to laboratory atmosphere. The 6H-SiC substrates (on-axis, resistivity 0.073 ohm-metre) were obtained from CREE Tech, the low-temperature effusion cell is supplied by SPECS Scientific Instrument, and the Mg shavings (99.98 % pure)

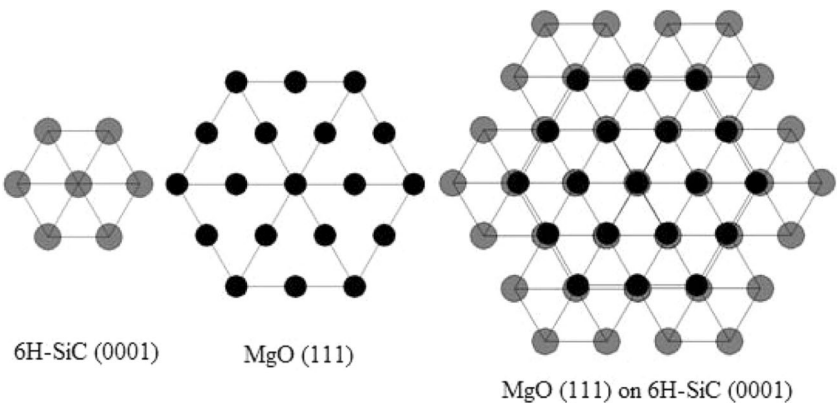

Fig. 1 Schematic of O bridge assisted growth of 30° rotated pseudo hexagon of MgO (111) on high-temperature hydrogen cleaned, silicate adlayer terminated and ($\sqrt{3} \times \sqrt{3}$) R30° reconstructed 6H-SiC (0001) surfaces

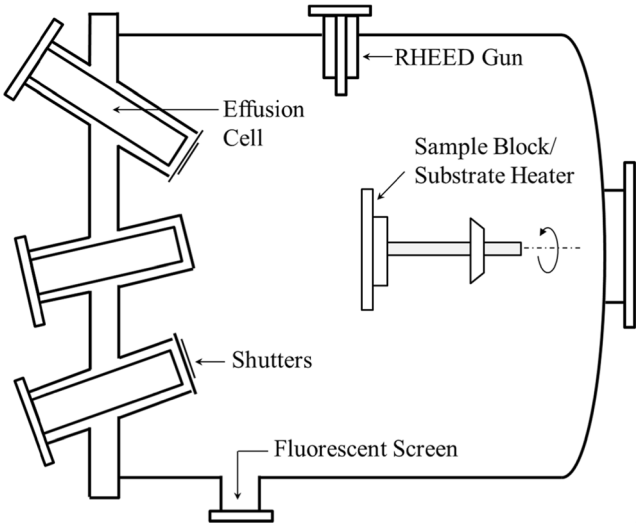

Fig. 2 Schematic of MBE growth chamber showing the equipment positioning

were purchased from Alpha Aesar. The O plasma is generated by the Oxford Applied Research Ltd. Remote oxygen RF-plasma source and the plasma intensity (mV) is measured by optical photodiode. The Mg source's temperature (°C) is measured by a thermal sensor positioned inside the effusion cell while the substrate's temperature (°C) is monitored using a back-face thermocouple installed in the substrate mount.

After cleaning the 6H-SiC substrates using an ex situ high-temperature hydrogen etching-based process, the substrates were transferred to the UHV chamber and characterized by RHEED and XPS prior to MgO film deposition. Epitaxial growth of MgO films is perfumed in situ by exposing the surface to Mg and O atomic species fluxes simultaneously. The details of the process were provided in an earlier publication [6].

3 Input process and output diagram

Figure 3 shows the input-process-output (IPO) diagram of the MBE process. The process control variables are shown on the left hand side, the noise factor on the top, and the key performance indicator on the right hand side of the process box. The measured values of the process control variables are likely to have minute variations (≈1 % of a desired setting). Plasma lighting is not a very precisely controllable variable. For a specific value of the plasma intensity, the plasma power may vary significantly, so it is considered an uncontrollable variable.

As the film is being deposited on a substrate, the quantity of the substrate-generated photoelectrons that reach the film-vacuum interface without energy loss decreases. This photoelectron attenuation is directly proportional to the thickness of the film being grown. By knowing specific properties (density, valence level, etc.) of the film, as well as the system geometry and electron energies, it is possible to estimate the film thickness from the degree of attenuation of photoelectrons emanating from the substrate. In this work, photoelectron intensity is measured in situ by XPS. In order to calculate the film thickness, Si2p3 scans were conducted both before and after the deposition of the MgO films on SiC substrates using Electron Effective-Attenuation-Length (EAL) Database or Standard Reference Database 82 provided by the National Institute of Standards and Technology (NIST) [2, 14, 15]. Figure 4 shows the relationship between the thickness of the MgO film in Angstroms, T_{Mgo}, and silicon signal attenuation, Si_{post} / Si_{pre}, where Si_{post} is the total area under the curve of the silicon (Si2p3) peak after the MgO is grown on the substrate and Si_{pre} is the total area under the curve of the silicon (Si2p3) peak before the MgO is grown on the substrate. The logarithmic best fit curve for the plot is given by $T_{MgO} = 1.0134 - 26.99 \ln (Si_{post} / Si_{pre})$. It has an R^2 value of 1. Here, R^2 is the coefficient of determination, which indicates the proportion of the variance in the dependent variable that is predictable from the independent variable.

The definitions of the process control variables and the key performance indicator are presented below.

Growth time (min) It is the time between opening and closing of the shutter in front of the substrate mount inside the chamber. The shutter allows or blocks the magnesium flux from reaching the surface of the substrate.

Substrate temperature (°C) It is the temperature measured by a thermocouple installed inside the substrate mount. It is measured by the electronic feedback control system installed on the MBE equipment.

Magnesium source temperature (°C) It is the temperature of magnesium chips measured by a temperature sensor positioned in the effusion cell. It is controlled by the electronic feedback control system installed on the equipment.

Atomic oxygen percentage on starting substrate surface It is the amount of oxygen on the surface of the SiC substrate after cleaning. It is measured by XPS analysis as a percentage of the overall chemical composition of the cleaned surface. The oxygen content on the starting surface is included as an input parameter because it strongly relates to the MgO film composition and structure.

Plasma intensity (mV) It is the intensity of the photons emitted by the cracked oxygen as measured by the optical emission detector (mV) installed on the remote oxygen source.

Plasma power (watts) It is the power applied to the RF-plasma source to convert oxygen gas into reactive atomic oxygen. This variable is kept constant for each experiment,

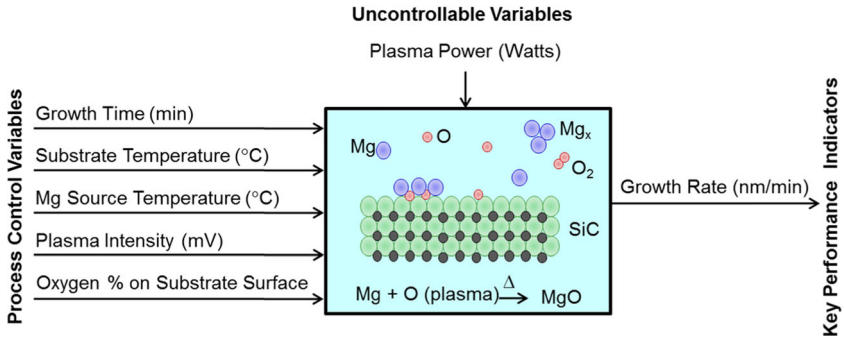

Fig. 3 Input-process-output (IPO) diagram for MBE process to grow MgO (111) nanoscale thin films on 6H-SiC (0001) substrates

and the drift in the value (watts) is manually adjusted to bring the variable back to its desired value in the experiment.

Growth rate (nm/min) It is computed by dividing the thickness (nm) of MgO film estimated using the EAL database by the growth time allowed for film growth.

4 Experimental data

Based on the authors' previous experience with analyzing MBE process [6, 7], a mixed level full factorial design of experiments was designed to study the correlations and associations between the critical process control variables and MgO film growth rate.

The control variables for the design of experiments are substrate temperature (two levels: 100 °C and 300 °C), magnesium source temperature (two levels: 328 °C and 350 °C), and plasma intensity (three levels: 0 mV, 305 mV, and 505 mV). Data was collected at these 12 combinations of substrate temperature, magnesium source temperature, and plasma intensity. For these 12 settings, percentage oxygen content of the starting surface varies randomly between 10 % and 13 % because it was hard to control these parameters precisely to a target value. Similarly, growth time varies between 3.75 minutes and 10 minutes because each experiment takes a different time period to complete. All the experiments were performed at a background chamber pressure (plasma pressure) of 6.666 × 10–4 Pa (or 5 × 10–6 Torr). The detailed design of experiments with specific values for each of the control variables is presented in Table 1. For example, run (treatment) 1 is conducted at substrate temperature of 100 °C, Mg source temperature of 328 °C, plasma intensity of 0 mV, and percentage starting oxygen of 0.1152. At this operating condition, growth time, film thickness, and growth rate were recorded as 5.00 minutes, 0.1024 nm, and 0.8889 nm/min, respectively. Plasma intensity varies during the growth experiment, so it was adjusted to keep it close to the desired values. During the experimentation, the plasma intensity varied between 300 and 310 mV for mid-level setting and 500 and 510 mV for max-level setting. Therefore, they are recorded as 305 and 505 mV, respectively.

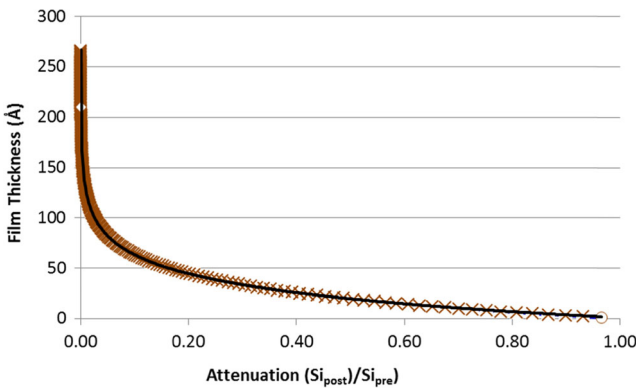

Fig. 4 Thickness versus attenuation plot based on EAL calculations

5 Neural network-based process model

From Table 1, it is obvious that there are 12 experimental runs. These experiments require a lot effort, time, and resources to conduct. However, 12 runs are not a sufficient basis for a response surface-based analysis. To address this limitation, an MBE process model of the form $y = f(x_1, x_2, \ldots, x_n) + \varepsilon$ from the experimental data was built. The process model was built such that it captures the response (growth rate y) behavior of the MBE process over the 4-dimensional covariate space defined by x_1 = substrate temperature (°C), x_2 = Mg source temperature (°C), x_3 = plasma intensity (mV), and x_4 = percentage starting oxygen. Here, ε represents the model residue term or estimation error. Considering that the relationship $y = f(x_1, x_2, \ldots, x_n) + \varepsilon$ between the response variable (y) and the covariates is highly nonlinear, a multilayer neural network model instead of a multiple linear regression model was used. A multilayer neural network is an appropriate model to estimate a functional form of a curved relationship, especially when the unknown function has complex shape which cannot be converted to a linear relationship by some transformation. Multilayer neural networks are an important class of highly connected feed-forward neural networks. They are well accepted as good approximation models of nonlinearities in the training data [8, 9].

Table 1 The design of experiments for the growth rate study

No.	Substrate temperature (°C)	Mg source temperature (°C)	Plasma intensity (mV)	% starting oxygen	Growth time (min)	Film thickness (nm)	Growth rate (nm/min)
1	100	328	0	11.5225	5.00	0.1024	0.8889
2	100	328	305	9.3099	5.00	0.0792	0.8503
3	100	328	505	10.9137	7.00	0.1135	1.0395
4	100	350	0	10.1568	10.00	0.0977	0.9616
5	100	350	305	10.7638	6.00	0.1496	1.3895
6	100	350	505	12.1559	4.00	0.2094	1.7227
7	300	328	0	10.4447	5.00	0.0353	0.3378
8	300	328	305	11.0679	5.00	0.0897	0.8104
9	300	328	505	12.4208	4.00	0.1775	1.4289
10	300	350	0	11.1137	4.00	0.0335	0.3012
11	300	350	305	11.0221	7.00	0.1741	1.5793
12	300	350	505	12.0204	3.75	0.1683	1.4001

A multilayer neural network contains feed-forward connections with a layer of input nodes, one or more layers of hidden nodes, and a layer of output nodes [16]. The input signal propagates forward layer-by-layer with every node in the hidden and output layers representing a smooth and differentiable nonlinear activation function. The number of hidden layers and the number of nodes in each layer are neural network architecture design parameters. The best neural network architecture was determined for this application by systematically varying these design parameters and then verifying the neural network performance in terms of accurately modeling the relationship between process input variables and response variable. Figure 5 presents the architecture of the neural network model selected for this application. It has four input nodes corresponding to four process variables (substrate temperature, magnesium source temperature, plasma intensity, and percentage starting oxygen) and one output node for the response variable (growth rate). In between input and output layer is an 11-node hidden layer.

The neural network was trained using the data from Table 1. This data set was randomly spilt into ten training records and two validation records. The network was trained with ten records and the training process was cross-validated with two remaining records. This process of splitting data and training the neural network was carried out many times to check the neural network training behavior.

Figure 6 presents the convergence of training error and validation error through thousands of training iterations. The neural work training and validation error kept converging up to 22,000 iterations, though with decreasing rate (see Fig. 6). Accordingly, the neural network was trained through 22,000 iterations using all 12 data sets listed in Table 1 to have a good data-driven model.

The scatter plot of the predicted versus the actual values for train data gave an R^2 value of 0.98. This confirms that the neural network model is able capture the response behavior of the MBE process well and the fit of the model is very good.

6 Response surface model

The neural network model was used to generate data for 3-level full factorial design on experiment with eleven replications for each run [6]. The settings for each run are given in Table 2. The neural network model was used to predict the responses for these runs.

Using this data, a response surface regression model was built for studying main effects and interaction effects of process control variables on the response variable. Both the R^2 and the adjusted R^2 values for response surface regression was 0.94, which indicates a desirable level of goodness of fit. Figure 7a presents the coefficients of the response surface regression model of the four input variables and one response variable.

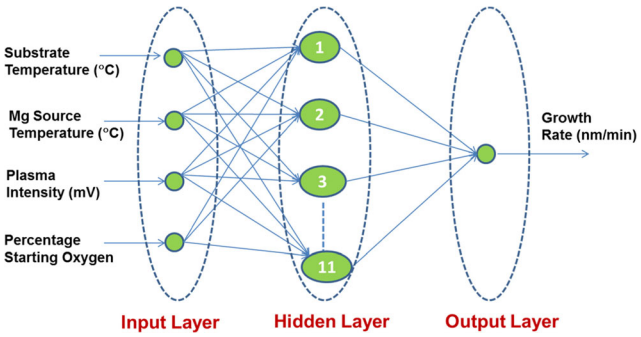

Fig. 5 Architecture of multilayer perceptron (MLP). It was trained to serve as a process model

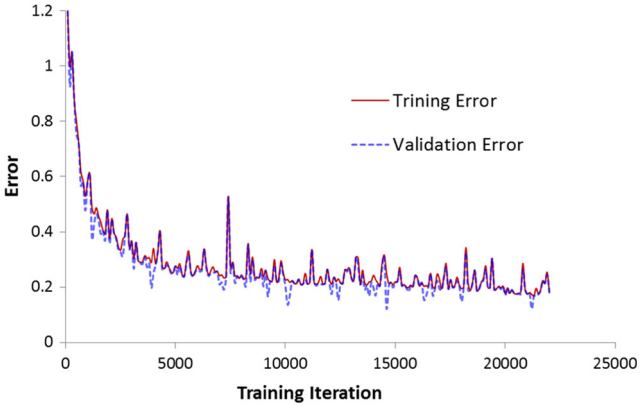

Fig. 6 MLP training and validation error convergence graph

7 Results and discussion

This section discusses (a) the effect of the individual process control variables on the growth rate using marginal mean plots; (b) the significance of individual process control variables, their quadratic terms, and their two- and three-way interactions to the growth rate using Pareto chart of coefficients; and (c) the effect of key critical variable interactions on the growth rate using response surface method.

7.1 Marginal mean plots and Pareto of coefficients

Figure 8 presents the marginal mean plots drawn from the response surface model.

The increasing substrate temperature slows down the growth rate of the film as shown in Fig. 8. However, the increase in magnesium source temperature, plasma intensity, and percentage starting oxygen content promotes the growth rate (Fig. 8). It is important to note that the rise in the starting oxygen content reduces the structural and chemical quality of the MgO film [6, 7]. The Pareto of response surface regression model coefficients (see Fig. 7b) reveals that the plasma intensity has the most significant influence on growth rate; both the main and quadratic terms have influence on growth rate. After the plasma intensity, in descending order, the variables that affect growth rate are the substrate temperature, percentage of starting oxygen, and magnesium source temperature. The growth rate also depends on interaction of substrate temperature, plasma intensity, and percentage starting oxygen on substrate surface. The interaction between the substrate temperature and plasma intensity is significant. However, this interaction needs to be further studied with respect to varying starting oxygen content. The response surface plots were employed to investigate this interaction at two levels of the two levels of the starting oxygen content.

Table 2 Settings for data generation for building response surface model

Variable	Min	Mid	Max
Substrate temperature	100	200	300
Mg source temperature	328	340	350
Plasma intensity	0	270	505
% starting oxygen	10	11	12

7.2 Response surfaces analysis

The optimum value for magnesium source temperature (340 °C) that delivers a highly crystalline and chemically stoichiometric (~1:1) MgO (111) film [9, 17, 18] for the response surface regression was used. In an earlier work [8], the authors labeled substrates as categories 1, 2, and 3 depending on the level of successful cleaning for elimination of starting oxygen content. The levels of starting oxygen content have been categorized based on the structural and chemical characterization and their impact on the quality of MgO thin films have been presented in the authors' earlier work [9, 19]. Category 1 represents the effectively cleaned and well-reconstructed samples with crisp second Lau rings on RHEED and an oxygen content between 7 % and 10% of the overall surface chemistry. Category 2 represents the ineffectively cleaned surface showing only the primary signs of ($\sqrt{3} \times \sqrt{3}$) R30° surface reconstruction with dim second Lau rings, and an oxygen content between 10 % and 12.5 % of the overall surface chemistry. Category 3 represents the poorly cleaned surface with no signs of the ($\sqrt{3} \times \sqrt{3}$) R30° reconstruction, and oxygen content above 13 % of the overall surface chemistry.

In the present work, the response surface at two different values of percentage starting oxygen, i.e., 10 % and 13% representing category 1 and category 3 of cleaned surfaces of the 6H-SiC substrates, respectively (Figs. 9 and 10) [8], was plotted. Category 1 substrates are the high-quality substrates with $\sqrt{3} \times \sqrt{3}$ R30° reconstructed 6H-SiC (0001) surface with optimum oxygen content. However, the category 3 substrates have excessive oxygen on the surface and high roughness [8].

Higher substrate temperatures slow down the film growth rate for both category 1 (good-quality film surface with O = 10 %) and category 3 (bad-quality film surface with O = 13 %) substrates especially at the low (0 mv -100 mV) and medium (100mV - 350 mV) values of the plasma intensity. Therefore, its impact on the growth reaction is independent of the reactivity of the oxygen. The minimum and maximum of growth rate values (nm/min) along the substrate temperature at 0 mV plasma intensity are ≈0.3 nm/min and 0.7 nm/min on a category 1 substrate and 0.5 nm/min and 1.1 nm/min on a category 3 substrate (Figs. 9 and 10).

Previous studies [9, 17–19] have shown that increased oxygen content on the starting surface leads to low-quality films; specifically, it results in the loss of the (111) single-crystal orientation necessary for integration of complex functional oxides. The excessive oxygen on the surface of the substrate in

Growth Rate = 1.0520 – 0.1301(A) + 0.0333(B)
+ 0.3002(C) + 0.1042(D) – 0.0003(AA)
– 0.0045(AB) + 0.0637(AC) – .0035(AD)
– 0.0012(BB) + 0.0110(BC) – 0.0024(BD)
– 0.1109(CC) – 0.0131(CD) - 0.0081(DD)
– 0.0002(ABC) – 0.0048(ABD)
+ 0.0319(ACD) – 0.0005(BCD)

A = Substrate temperature
B = Magnesium source temperature
C = Plasma intensity
D = Percentage starting oxygen

A

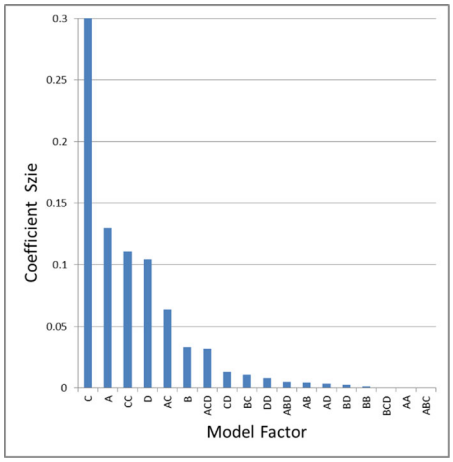

B

Fig. 7 **a** Response surface regression model for growth rate (nm/min). **b** Pareto of model factors base their coefficient size

Fig. 10, especially along the increasing substrate temperature, indicates that the O–O bridge formation at the interface of the film and substrate, which controls the alignment of the 111-orinetaion, is what slows down the growth rate in the initial stages of the deposition. At the growth of the first few monolayers, the growth rate would be slow during the interface formation between the pseudo hexagons of $\sqrt{3} \times \sqrt{3}$ R30° reconstructed 6H-SiC (0001) and MgO (111).

Therefore, the growth of high-quality MgO (111) nanoscale thin films would always face a two-stage growth rate situation. If there is excessive oxygen on the starting surface of substrate (13 % and more), the film loses the (111) characteristic but grows much faster. There is trade-off between growth rate and film quality. It is important to note that growth rate must be weighed against the quality of the films grown. As this study provides a collective view of deposition process, what remains as an unexplored possibility is the impacts of different process variables on the first versus the second stage of this two-stage film growth process.

Plasma intensity clearly has a significant impact on growth rate irrespective of the percentage starting oxygen on the surface of the substrate. The stronger gradients along the plasma intensity at the higher side of the substrate temperature (Figs. 9 and 10) suggest that the reactivity of the oxygen drives the growth rate of MgO nanoscale thin films. However, the min and max values of the growth rate along plasma intensity at lower substrate temperature for category 1 substrate surface are 0.7 nm/min and 1.3 nm/min and 1.1 nm/min and 1.5 nm/min for category 3 substrate. This again suggests that the growth of high-quality film is slower than the low-quality films grown on category 3 substrates. Moreover, the high-quality films grow faster at higher values of plasma intensity (300 mV and above) and lower values of substrate temperature (100 °C - 150 °C). If crystallinity is not a quality goal, then increasing the plasma power on a high oxygen-content substrate will significantly increase growth rate of MgO film.

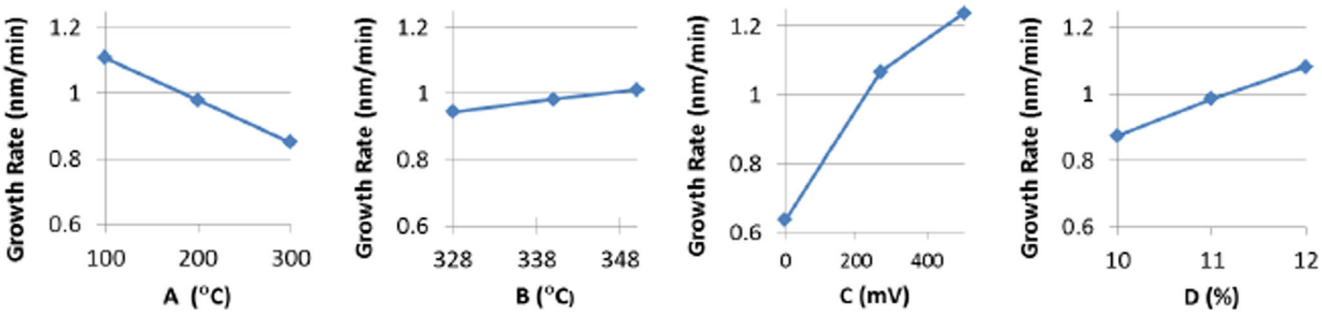

Fig. 8 Marginal mean plots for main effects of process input variables (*A* = substrate temperature, *B* = magnesium source temperature, *C* = plasma intensity, and *D* = percentage starting oxygen)

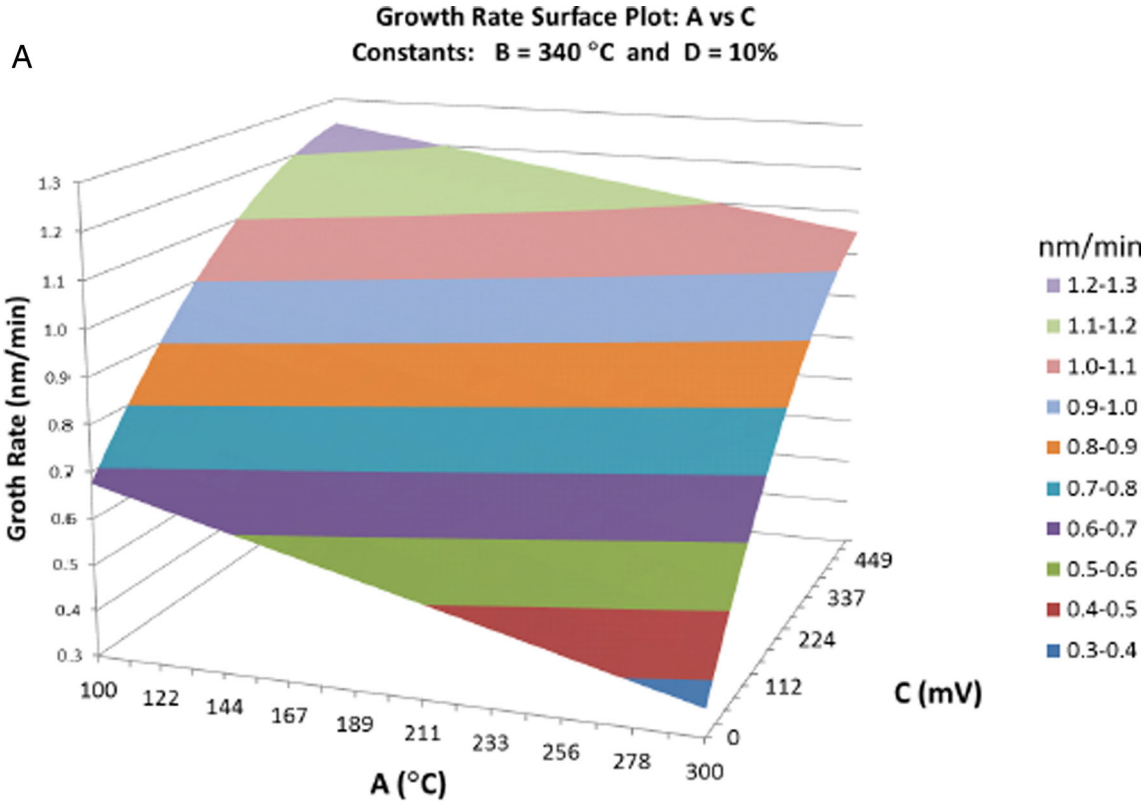

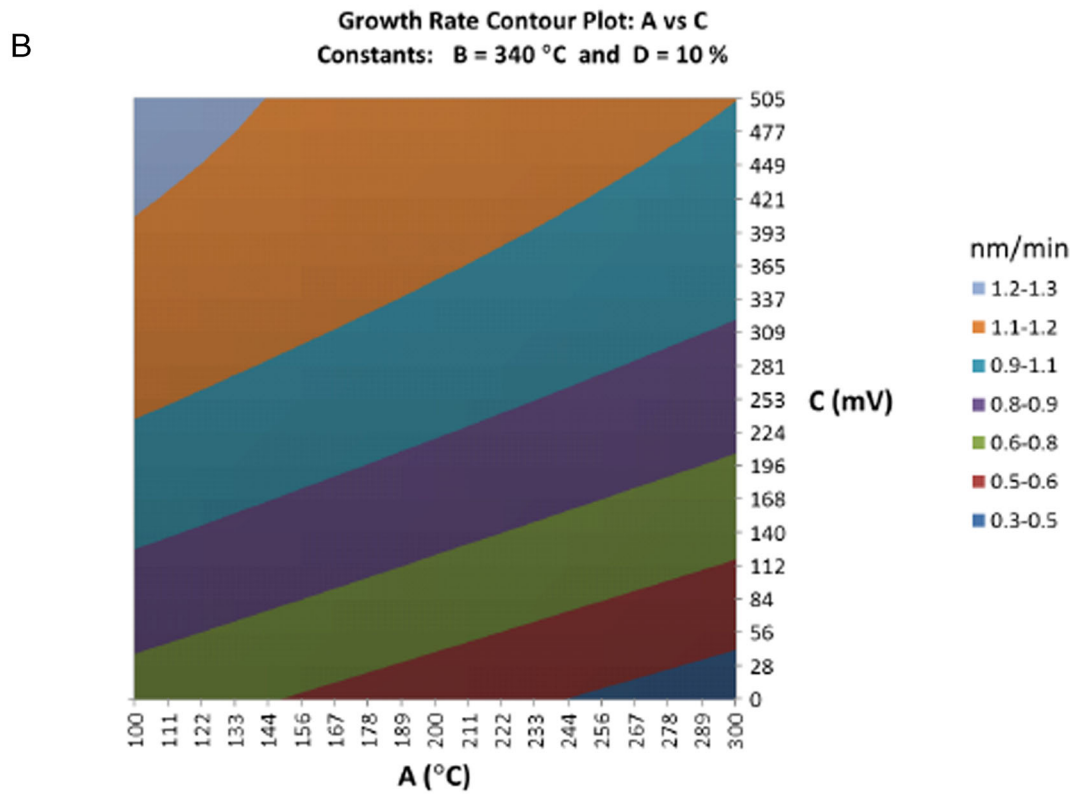

Fig. 9 Interaction between substrate temperature and plasma intensity at two levels starting oxygen on substrate surface. **a** Response surface at $B = 340$ °C and $D = 10$ %. **b** Response surface at $B = 340$ °C and $D = 13$ %; (A = substrate temperature, B = magnesium source temperature, C = plasma intensity, and D = percentage starting oxygen)

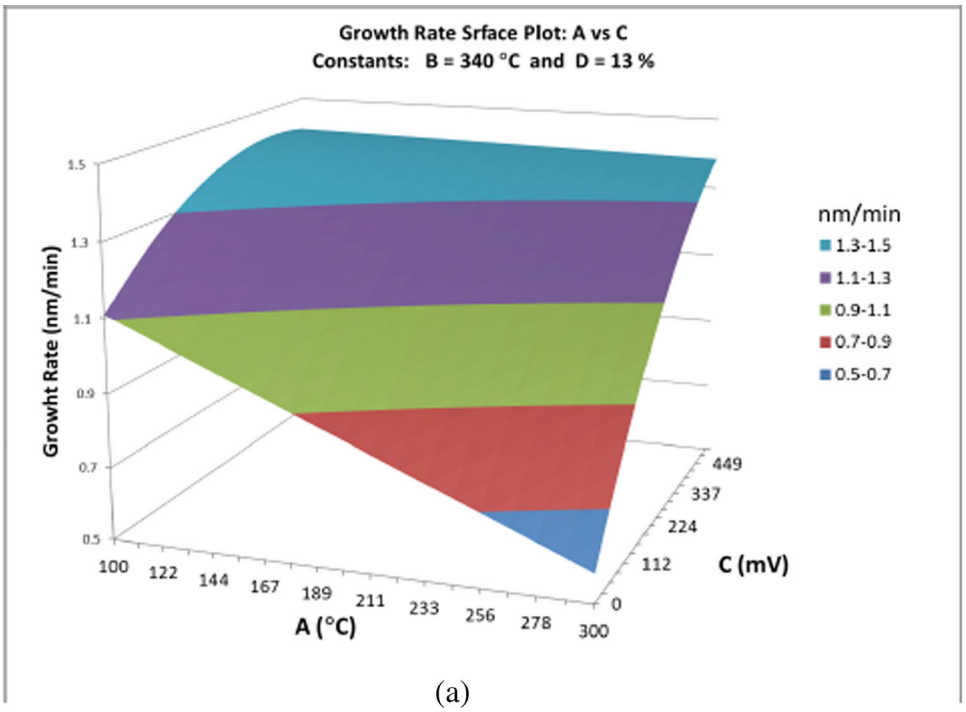

(a)

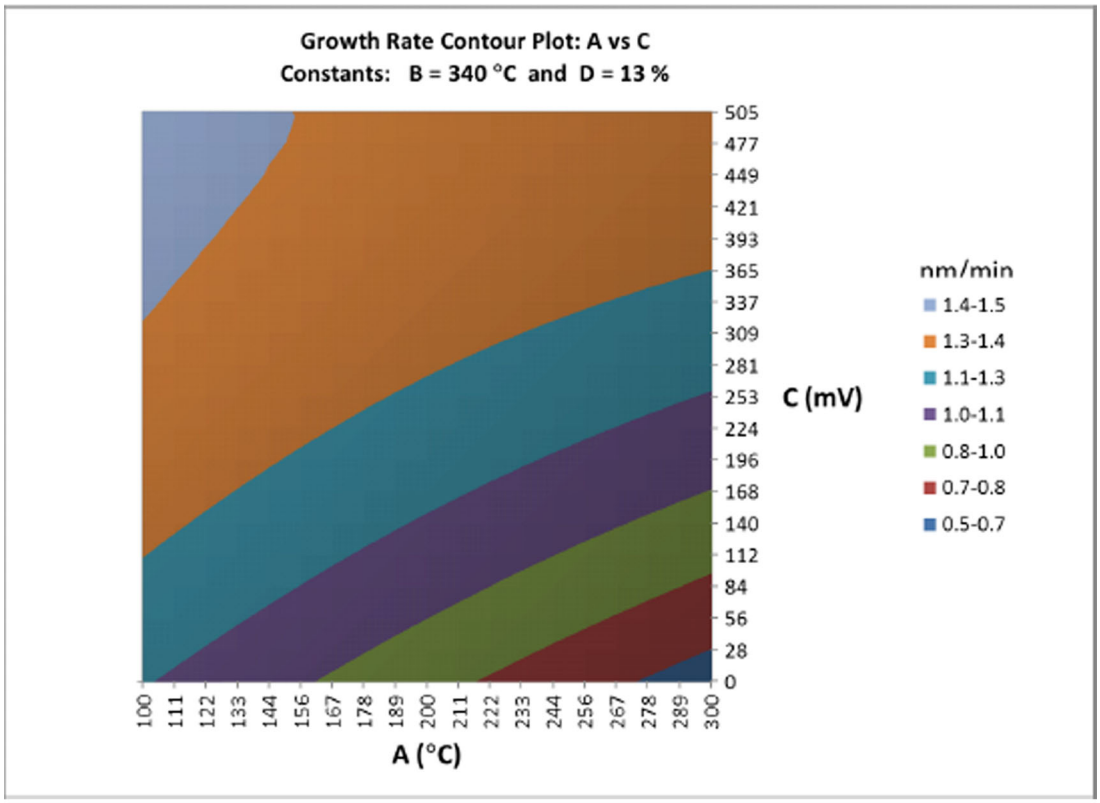

(b)

Fig. 10 Interaction between substrate temperature and plasma intensity at two levels starting oxygen on substrate surface at B = 340 °C and D = 13%: **a** response surface at B = 340 °C and D = 10% and **b** response surface at B = 340 °C and D = 13%. A substrate temperature, B magnesium source temperature, C plasma intensity, D percentage starting oxygen)

8 Conclusions

To summarize, the response surface regression model suggests that for the ranges of control variables in the MgO study, i.e., magnesium source temperature 340 °C, plasma intensity 350 mV - 400 mV, and substrate temperature 140 °C - 200 °C, the growth rate would follow a two-stage phenomenon on category 1 substrates with growth rate between 0.7 nm/min and 1 nm/min. For the same ranges of control variables, the growth rate would be between 0.9 nm/min and 1.3 nm/min for category 3 substrates. The study of variations in band gap with respect to the different thicknesses of MgO nanoscale thin films grown on category 1 and category 3 substrates needs to be investigated to extend on the present work. In addition, the deconvolution of the mechanisms during the first and second stage of high-quality film growth could lead to a process control scheme that would ensure good quality through a slower first stage, and then increase growth rate while maintaining quality in the second stage.

Acknowledgements The authors thank the National Institute of Standards and Technology for providing funding for this research under sponsor award number 70NANB15H028.

Compliance with ethical standards

Disclaimer Certain commercial software or equipment is identified in this article in order to aid understanding. Such identification does not imply recommendation or endorsement by the National Institute of Standards and Technology, nor does it imply that the materials or equipment identified are necessarily the best available for the purpose.

References

1. Doolittle WA, Carver AG, Henderson W (2005) Molecular beam epitaxy of complex metal-oxides: where have we come, where are we going, and how are we going to get there? Journal of Vacuum Science & Technology, B: Microelectronics and Nanoscalemeter Structures-Processing, Measurement, and Phenomena 23(3): 1272–1276
2. Goodrich TL (2008) *Atomistic investigation into the interface engineering and heteroepitaxy of functional oxides on hexagonal silicon carbide through the use of a magnesium oxide template layer for the development of a multifunctional heterostructure*, Dissertation, Northeastern University
3. Craft HS, Ihlefeld JF, Losego MD, Collazo R, Sitar Z, Maria J-P (2006) MgO epitaxy on GaN (0002) surfaces by molecular beam epitaxy. Appl Phys Lett 88(21):212906.1–212906.3
4. Chen Z, Yang A, Geiler A, Harris VG, Vittoria C, Ohodnicki PR, Goh KY, McHenry ME, Cai Z, Goodrich TL, Ziemer KS (2007) Epitaxial growth of M-type Ba-hexaferrite films on MgO (111) SiC (0 0 01) with low ferromagnetic resonance linewidths. Appl Phys Lett 91(18):182505.1–182505.3
5. Cai Z (2010) *Molecular beam epitaxy integration of magnetic ferrites with wide bandgap semiconductor 6H-SiC for next generation microwave and spintronic devices*, Dissertation, Northeastern University
6. Goodrich TL, Cai Z, Ziemer KS (2008) Stability of MgO(111) films grown on 6H-SiC(0001) by molecular beam epitaxy for two-step integration of functional oxides. Appl Surf Sci 254:3191–3199
7. Goodrich TL, Cai Z, Losego MD, Maria J-P, Kourkoutis LF, Muller DA, Ziemer KS (2008) Improved epitaxy of barium titanate by molecular beam epitaxy. Journal of Vacuum Science Technology B 26:024803
8. Cai Z, Chen Z, Goodrich TL, Harris VG, Ziemer KS (2007) Chemical and structural characterization of barium hexaferrite films deposited on 6H-SiC with and without MgO/BaM interwoven layers. J Cryst Growth 307:321
9. Uddin GM, Ziemer KS, Zeid A, Kamarthi S (2012) "Study of lattice strain propagation in molecular beam epitaxy of nanoscale scale magnesium oxide thin film on 6H-SiC substrates using neural network computer models." Proceedings of the International Mechanical Engineering Congress and Exposition Houston, Texas, USA
10. Bernhardt J, Schardt J, Starke U, Heinz K (1999) Epitaxially ideal oxide semiconductor interfaces: silicate adlayers on hexagonal (0001) and (000-1) SiC surfaces. Appl Phys Lett 74:1084–1086
11. Ramachandran V, Brandy MF, Smith AR, Feenstra RM, Greve DW (1996) Preparation of atomically flat surfaces on silicon carbide using hydrogen etching. J Electron Mater 27:308–312
12. Goodrich TL, Parisi J, Leong J, Ziemer KS (2005) "SiC surface preparation by hydrogen cleaning for high-temperature, high-power device integration," Proceedings of AICHE Annual Meeting, Cincinnati, OH, p. 135
13. Lazarov VK, Cai Z, Yoshida K, Zhang KH, Weinert M, Ziemer KS, Hasnip PJ (2011) Dynamically stabilized growth of polar oxides: the case of MgO(111). Phys Rev Lett 107(5):056101
14. Nation Institute of Standards and Technology Standard's Reference Database 82, https://www.nist.gov/srd/nist-standard-reference-database-82
15. Wagner CD, Riggs WM, Davis LE, Moulder JF, Muilenberg GE (1979) Handbook of X-ray photoelectron spectroscopy: Perkin-Elmer Corporation, NIST
16. Haykins SP (2009) Neural networks and learning machines. Prentice Hall/Pearson, New York
17. Uddin GM, Cai Z, Ziemer KS, Zeid A, Kamarthi S (2010) Analysis of molecular beam epitaxy process for growing nanoscalescale magnesium oxide films. ASME Journal of Manufacturing Science and Engineering 132(3):030913.1–030913.9
18. Uddin GM, Ziemer KS, Zeid A, Kamarthi S (2015) Monte Carlo study of the molecular beam epitaxy process for manufacturing magnesium oxide nano-scale films. IIE Trans 47:125–140
19. Uddin GM, Ziemer KS, Zeid A, Kamarthi S (2013) Monte Carlo study of the high temperature hydrogen cleaning process of 6H-silicon carbide for subsequent growth of nano scale metal oxide films. International Journal of Nanoscalemanufactruing 9(5/6):407–430